Supporting Information for

HKDC1, a target of TFEB, is essential to maintain both mitochondrial and lysosomal homeostasis, preventing cellular senescence

Mengying Cui, Koji Yamano, Kenichi Yamamoto, Hitomi Yamamoto-Imoto, Satoshi Minami, Takeshi Yamamoto, Sho Matsui, Tatsuya Kaminishi, Takayuki Shima, Monami Ogura, Megumi Tsuchiya, Kohei Nishino, Brian T Layden, Hisakazu Kato, Hidesato Ogawa, Shinya Oki, Yukinori Okada, Yoshitaka Isaka, Hidetaka Kosako, Noriyuki Matsuda, Tamotsu Yoshimori*, Shuhei Nakamura*

* Correspondence: tamyoshi@fbs.osaka-u.ac.jp (T.Y.), shuhei.nakamura@naramed-u.ac.jp (S.N.)

This PDF file includes:

Supporting Information Text

SI Materials and Methods

Antibodies

The following antibodies were used: anti-HKDC1 (25874-1-AP, Proteintech) (1:400 for WB); anti-GAPDH (2118, Cell Signaling Technology) (1:80000 for WB); anti-TOM20 (sc-11415, Santa Cruz Biotechnology) (1:1000 for WB and IF); anti-UQCRC1 (459140, Invitrogen) (1:2000 for WB); anti-FK2 (0918-2, Nippon Bio-Test Laboratories) (1:1000 for IF to detect Ub); anti-pUb (62802, Cell Signaling Technology) (1:1000 for WB); anti-Parkin (2132, Cell Signaling Technology) (1:1000 for WB); anti-PINK1 (LS-C96472-100, LSBio) (1:400 for WB); anti–c-Myc (626802, BioLegend) (1:1000 for IF); anti-mNG (53061, Cell Signaling Technology) (1:1000 for WB); anti-FLAG (F1804, Sigma) (1:500 for WB, IF and PLA); anti-TOM70 (sc-390545, Santa Cruz Biotechnology)(1:1000 for WB and PLA); anti-TFEB (4240, Cell Signaling Technology) (1:1000 for WB); anti-Gal3 (sc-23938, Santa Cruz Biotechnology) (1:1000 for IF); anti-CHMP4B (13683-1-AP, Proteintech) (1:1000 for IF); anti-ALIX (D38G5, #8168) (1:1000 for IF); anti-VPS4 (SAB4200025, Sigma) (1:1000 for IF); anti-CHMP2B (12527-1-AP, Proteintech) (1:1000 for IF); anti-p62 (pM045, MBL) (1:1000 for IF); anti-GFP (2555, Cell Signaling Technology) (1:1000 for PLA); anti-VDAC1 (sc-390996, Santa Cruz Biotechnology) (1:1000 for PLA); anti-LAMP1 (sc-20011, Santa Cruz Biotechnology) (1:1000 for IF); anti-LC3B (PM036, MBL) (1:1000 for WB); anti-p21 (ab109199, Abcam) (1:1000 for WB); anti-p16 (11104, IBL) (1:100 for WB); Peroxidase-AffiniPure Goat Anti–Rabbit IgG (H+L) (111-035-003, Jackson ImmunoResearch) (1:10000 for WB); Peroxidase-AffiniPure Goat Anti–Mouse IgG (H+L) (115-035-003, Jackson ImmunoResearch) (1:10000 for WB); Goat Anti–Rabbit IgG H&L, Alexa Fluor 568 (ab175695, Abcam) (1:1000 for IF); Goat Anti–Mouse IgG H&L, Alexa Fluor 647 (ab150073, Abcam) (1:1000 for IF); Goat Anti–Mouse IgG (H+L) Cross-Adsorbed Secondary Antibody, Alexa Fluor 568 (A-11004, Invitrogen) (1:1000 for IF); Goat Anti–Rabbit IgG (H+L) Highly Cross-Adsorbed Secondary Antibody, Alexa Fluor 647 (A-21245, Invitrogen) (1:1000 for IF); Goat Anti–Rat IgG (H+L) Cross-Adsorbed Secondary Antibody, Alexa Fluor 488 (A-11006, Invitrogen) (1:1000 for IF); Goat Anti–Rat IgG (H+L) Cross-Adsorbed Secondary Antibody, Alexa Fluor 568 (A-11077, Invitrogen) (1:1000 for IF); Goat Anti–Rabbit IgG H&L, Alexa Fluor 488 (ab150085, Abcam) (1:1000 for IF); and Goat Anti–Mouse IgG H&L, Alexa Fluor 488 (ab150117, Abcam) (1:1000 for IF).

Plasmid construction

Plasmids containing pEYFP-N1-PINK1 (plasmid no. 101874) and SPLICS Mt-ER Short P2A (plasmid no. 164108)(1)were obtained from Addgene. Human HKDC1, VDAC2, and VDAC3 PCR amplification was conducted using the following primers: HKDC1 (5'-TCAGTCGACTGGATCATGTTTGCGGTCCACTTGATGG-3' and 5'-GTCTAGATATCTCGAGTTCTCCTTCTGTGCCTGCTG-3'), VDAC2 (5'-CAGTCGACTGGATCCATGAGCTGGTGTAATGAGCTCAGATTGC-3' and 5'-TGGGTCTAGATATCTAGCCTCCAACTCCAGGGCGAG-3'), and VDAC3 (5'-CAGTCGACTGGATCCATGTGTAACACACCAACGTACTGTGAC-3' and 5'-TGGGTCTAGATATCTAGCTTCCAGTTCAAATCCCAAGCC-3'), followed by an In-Fusion reaction (639649, Takara Bio). Human TOM70, VDAC1, and TRPML1 cDNA fragments were amplified using the following primers and then cloned into the KpnI/XhoI, BamHI/EcoRV, or BamHI/NotI site of the pENTR vector: TOM70 (5'-TTTTGGTACCACTTGTCATGGCCGCCTCTAAA-3' and 5'-TTTTCTCGAGTGTAATGTTGGTGGTTTTAATCCGTATTTCT-3'), VDAC1 (5'-AAAAGGATCCATGGCTGTGCCACCCACGTA-3' and 5'-ATCTTGCTTGAAATTCCAGTCCTAGACCAAGCT-3'), and TRPML1 (5'-TCAGTCGACTGGATCCCTACAGCCCCGGCGGGTCC-3' and 5'-ATCTCGAGTGCGGCCGCTCAATTCACCAGCAGCGA-3'). PINK1-EYFP was subcloned from pEYFP-N1-PINK1 into the XhoI/NotI site of the pENTR vector. PINK1 was subcloned from pMRX-PINK1-EYFP into the BamHI/EcoRI site of the pBABE-puro_TEV-3xFLAG vector (2). LAMP1 was subcloned from pENTR-1A-LAMP1 (3) into the BamH1/EcoRV site of SPLICs Mt-ER Short P2A to replace the sequence of ER(Sac1 MTS). SPLICS LAMP1-MT Short P2A ($SPLICS^{LY\text{-}MT}$) was then subcloned into BamHI/XbaI site of pENTR vector (shown in Figure 5F). HKDC1 and PINK1 mutants were generated by site-directed mutagenesis using the following primers: ΔN20 HKDC1 (5'-GTCGACTGGATCATGAAGGTGGACAGGTTC-3' and 5'-GAACCTGTCCACCTTCATGATCCAGTCGAC-3'), S155A HKDC1 (5'-CTTGGCCTAACTTTTGCTTTCCCCTGTCGAC-3' and 5' GTCGACAGGGGAAAGCAAAAGTTAGGCCAAG-3'), S602A HKDC1 (5'-TTGGGCTTCACATTCGCATTTCCCTGCAGGC-3' and 5'-GCCTGCAGGGAAATGCGAATGTGAAGCCCAA-3'), N20 HKDC1 (5'-GAGGACCAGATCAAGTCGAGATATCTAGAC-3' and 5'-

GTCTAGATATCTCGACTTGATCTGGTCCTC-3'), ΔN34 PINK1 (5'-AAGCTTGCCACCATGGGCCCGGCGGCGGG-3' and 5'-CCCGCCGCCGGGCCCATGGTGGCAAGCTT-3'), ΔN93 PINK1 (5'-AAGCTTGCCACCATGGGCCCTTGCGGCCG-3' and 5'-CGGCCGCAAGGGCCCATGGTGGCAAGCTT-3'), ΔTMD PINK1 (5'-GCCTGGGGCTGCGCGATCGAGGAAAAACAG-3' and 5'-CTGTTTTTCCTCGATCGCGCAGCCCCAGGC-3'), and F104M PINK1 (5'-GCAGTCTTTCTGGCCATGGGGCTAGGGCTGGGC-3' and 5'-GCCCAGCCCTAGCCCCATGGCCAGAAAGACTGC-3'). TOM20TMD HKDC1 was produced by the In-Fusion reaction between the N-terminal 33 amino acid of TOM20 PCR amplification as insert (using the following primers: 5'-TCAGTCGACTGGATCATGGTGGGCCGGAACA-3' and 5'-GAACCTGTCCACCTTGTTGGGGTCACTCCGCCTTT-3') and the ΔN20 HKDC1 PCR amplification as vector (using the following primers: 5'-AAGGTGGACAGGTTCCTGTATCAC-3' and 5'- GATCCAGTCGACTGAATTGGTTCC-3'). pcDNA3.1 and pMRX-IRES-blast (pMRX-ib) plasmids were used as donor vectors for recombination-based cloning with the Gateway system (11791-020, Invitrogen). Recombinant retroviruses were prepared as previously described to generate stable cell lines (4).

RNA isolation and qPCR with reverse transcription

Isolation of total RNA and the cDNA synthesis were performed using the RNeasy Plus Mini Kit (74134, QIAGEN) and iScriptTM cDNA Synthesis Kit (1708891, Bio-Rad), respectively. qPCR was performed using Power SYBR Green PCR Master Mix (4367659, Thermo Fisher Scientific) and QuantStudio Real-Time PCR Software version 1.3. (Thermo Fisher Scientific). Primer sequences were as follows: human HKDC1 (5'-TGTGCCTATGACGACCCCTACT-3' and 5'-CACGCATTGGTGCCAGTTC-3'), human HK1 (5'-CCTTTGGAGACGATGGATCATT-3' and 5'-CCCGGTCTATCTCCCTGTCA-3'), human HK2 (5'-GAGCCATCCTGCAACACTTAGG-3' and 5'-CAGTGCACACCTCCTTAACAATG-3'), human PINK1 (5'-AGGCGTGGACCATCTGGTT-3' and 5'-GATGTTGTCGGATTTCAGGTCTCT-3'), human IL-1α (5'-AACCAGTGCTGCTGAAGGA-3' and 5'-TTCTTAGTGCCGTGAGTTTCC-3'), human IL-1β (5'-CTGTCCTGCGTGTTGAAAGA-3' and 5'-TTGGGTAATTTTTGGGATCTACA-3'), human GAPDH (5'-

TGCACCACCAACTGCTTAGC-3' and 5'-GGCATGGACTGTGGTCATGAG-3'), mouse HKDC1 (5'-AGCTGGTCAGGCTTATCTTGCT-3' and 5'-AGGATTTTGCACCCCCAAAC-3'), and mouse β-ACTIN (5'-TGGCTCCTAGCACCATGAAGATC-3' and 5'-CTGTCCACCTTCCAGCAGATGT-3').

RNA-seq

RNA sequencing was performed at the Center of Medical Innovation and Translational Research of Osaka University. RNA-seq libraries were prepared using the TruSeq Stranded mRNA Library Prep Kit (20020594, Illumina). Quality and quantity were assessed at each stage by capillary electrophoresis (Agilent Bioanalyzer and Agilent TapeStation). Libraries were quantified by qPCR, immobilized, and processed onto a flow cell with a cBot system (Illumina), followed by sequencing-by-synthesis with NovaSeq 6000 S4 chemistry on aNovaSeq 6000 at Macrogen-Japan. Reads were pre-processed using Trimmomatic (v0.35)(5). Alignment of the reads was done using TopHat (v2.1.1, for mitochondrial damage)(6) or Salmon (for lysosomal damage). The Bioconductor package, edgeR (for mitochondrial damage)(7), or DESeq2 (for lysosomal damage) was used to perform normalization and significance testing.

Transfection of siRNA

The siRNA duplex oligomers for Luciferase, HKDC1, TOM70, and VDAC3 were designed as follows as respectively: Luciferase: 5′-UCGAAGUAUUCCGCGUACG-3′, HKDC1: 5′-GGAGCUCUUUGAUCACAUU-3′, HKDC1#2: 5′-CCAUCAAGAGGAGAAACGA-3′, TOM70: 5′-CACUAUACGCCCAGGCAUU-3′, VDAC3: 5′-CAGGCAACCUAGAAACCAA-3′. The siRNAs for LONP1, CLPP, YME1L1, AFG3L2, SPG7, PARL, OMA1, VDAC1, and VDAC2 were purchased from Sigma. The siRNA for TFEB was purchased from Dharmacon. The siRNAs were transfected into cells using Lipofectamine RNAiMAX (13778150, Invitrogen). The transfected cells were used for the subsequent experiment after 48 h. The silencing efficiency was assessed by either WB or qPCR.

Cell fractionation

We separated the mitochondria-rich fraction from healthy or A/O treated HeLa cells by using the mitochondria isolation kit for cultured cells (89874, Pierce) following the manufacturer's instructions. The cytosol-rich fraction and mitochondria-rich fraction were harvested and analyzed by western blotting.

Western blotting

Cells were lysed in sample buffer containing 56 mM Tris-HCl (pH 6.8), 6% (v/v) glycerol, 2% SDS, 0.1 M DTT, and 2.4% Bromophenol Blue followed by heating at 95°C for 5 min. Protein concentrations were measured with the Protein Quantification Assay kit (740967.250, Macherey-Nagel). Samples were subjected to SDS–PAGE and transferred to polyvinylidene fluoride membranes (IPVH00010, Merck Millipore). The membranes were blocked with TBST (Tris-buffered saline and 0.1% Tween-20) containing 3% skim milk and incubated overnight at 4°C with primary antibodies diluted in blocking solution. The membranes were washed three times with TBST, incubated for 1 h at room temperature with 10,000× dilutions of HRP-conjugated secondary antibodies in blocking solution, and washed three times with TBST. The immunoreactive bands were detected using Immobilon Forte Western HRP substrate (WBLUF, Millipore) or ImmunoStar LD (290-69904, FUJIFILM Wako Chemicals) on a ChemiDoc Touch imaging system (Bio-Rad).

ChIP-qPCR assay

We performed ChIP-qPCR assays of HeLa cells overexpressing TFEB-3xFLAG or 3xFLAG as previously described(8). Briefly, after cross-linking cells with 1% paraformaldehyde (43368, Alfa Aesar) for 10 min at room temperature, cells were rinsed twice with cold PBS and then lysed in lysis buffer containing 50 mM Tris-HCl (pH 8.0), 10 mM EDTA, 1% SDS, and Protease Inhibitor Cocktail (11836170001, Roche), followed by incubation for 10 min at room temperature. The chromatin was sheared by sonication to generate DNA fragments of average lengths between 300 bp and 500 bp. For immunoprecipitation, chromatin was incubated with anti-FLAG antibody (F1804, Sigma) and Dynabeads Protein G (1004D, Invitrogen) overnight at 4°C. After washing and elution, the cross-linking was disrupted by heating overnight at 65°C, and DNA fragments were purified using the QIAquick PCR Purification Kit (28104, QIAGEN). Purified DNA was analyzed by qPCR. The primer sequences were as follows: human HKDC1 TSS -3000 (5’-CCAAATGCATGTGATCTCTGTAATC-3’ and 5’-CGTCTACATTCCAGGCCTGAGT-3’) and human HKDC1 TSS -10000 (5’-TGGCACTGACTCTATTTCCTCC-3’ and 5’-GAGATAAGCCCTTCCAGGCA-3’).

Immunofluorescence staining

Cells were fixed with 4% paraformaldehyde (09154-85, Nacalai Tesque) for 10 min, washed twice with PBS, permeabilized with 50 μg/mL digitonin in PBS for 10 min, blocked with 0.1% gelatin in PBS for 30 min, and then incubated with the indicated primary antibodies in 0.1% gelatin-PBS for 1 h, followed by incubation with fluorescence-conjugated secondary antibodies with or without DAPI (1:1000) and CellMask Deep Red Plasma Membrane Stain (1:100000, C10046, Invitrogen) in 0.1% gelatin-PBS for 40 min. All steps above were performed at room temperature. After secondary antibody treatment, the samples were observed on a CQ1 (Yokogawa) or FV3000 (Olympus) confocal microscope equipped with CQ-1 software (version 1.07.01.01) or FV31S-SW software (version 2.3.1.163), respectively.

Structural comparison and representation

The HKDC1 and HK2 structures were aligned using 5133 atoms from their respective models, resulting in a 0.76 Å root mean square deviation; the former was predicted by AlphaFold2 (AF-Q2TB90-F1-model_v4) (9, 10), while the latter was solved by X-ray crystallography (PDB ID: 2NZT)(11). The PyMOL Molecular Graphics System (Version 2.5.4, Schrödinger, LLC.) was employed.

Immunoprecipitation and mass spectrometry (MS)

Cells stably expressing FL HKDC1–mNG or △N20 HKDC1–mNG proteins were grown in a 10-cm dish and treated with or without A/O for 3 h, then cross-linked with 0.1% formaldehyde (063-04815, FUJIFILM Wako Chemicals) for 10 min at room temperature. After cross-linking was quenched with 100 mM glycine for 4 min at room temperature, cells were washed with HEPES saline containing 20 mM HEPES-NaOH buffer (pH 7.5) and 137 mM NaCl, and lysed on ice in HEPES-RIPA buffer containing 20 mM HEPES-NaOH buffer (pH7.5), 150 mM NaCl, 1 mM EGTA, 1 mM $MgCl_2$, 0.25% (w/v) Na-deoxycholate, 0.05% SDS, 1% (v/v) NP-40, 0.2% (v/v) Benzonase Nuclease (70746, Millipore), (4906837001, Roche), and Protease Inhibitor Cocktail.

After sonication and centrifugation at 20380 x g at 4°C for 15 min, the supernatants were incubated with mNG-Trap magnetic agarose beads (ntma-20, ChromoTek) at 4°C for 2 h. The beads were washed four times with HEPES-RIPA buffer and then twice with 50 mM ammonium bicarbonate. Proteins on the beads were digested by adding 200 ng trypsin/Lys-C mix (Promega) at 37°C overnight. The resultant digests were reduced, alkylated, acidified, and desalted using GL-Tip SDB. The eluates were evaporated and

dissolved in 0.1% trifluoroacetic acid and 3% acetonitrile (ACN). Liquid chromatography–MS/MS analysis of the resultant peptides was performed on an EASY-nLC 1200 UHPLC connected to an Orbitrap Fusion mass spectrometer through a nanoelectrospray ion source (Thermo Fisher Scientific). The peptides were separated on a C18 reversed-phase column (75 μm x 150 mm; Nikkyo Technos) with a linear 4–32% ACN gradient for 0–100 min, followed by an increase to 80% ACN for 10 min and a final hold at 80% ACN for 10 min. The mass spectrometer was operated in data-dependent acquisition mode with a maximum duty cycle of 3 s. MS1 spectra were measured with a resolution of 120,000, an automatic gain control (AGC) target of 4e5, and a mass range of 375–1,500 m/z. HCD MS/MS spectra were acquired in the linear ion trap with an AGC target of 1e4, an isolation window of 1.6 m/z, a maximum injection time of 35 ms, and a normalized collision energy of 30. Dynamic exclusion was set to 20 s. Raw data were directly analyzed against the SwissProt database restricted to *Homo sapiens* using Proteome Discoverer 2.5 (Thermo Fisher Scientific) with the Sequest HT search engine. The search parameters were as follows: (a) trypsin as an enzyme with up to two missed cleavages; (b) precursor mass tolerance of 10 ppm; (c) fragment mass tolerance of 0.6 Da; (d) carbamidomethylation of cysteine as a fixed modification; and (e) acetylation of the protein N-terminus and oxidation of methionine as variable modifications. Peptides were filtered at a false discovery rate of 1% using the Percolator node. Label-free quantification was performed on the basis of the intensities of precursor ions using the Precursor Ions Quantifier node. Normalization was performed such that the total sum of abundance values for each sample over all peptides was the same.

Immunoprecipitation for western blotting

For mNG-Trap agarose beads (nta-20, ChromoTek) immunoprecipitated assay, after sonication and centrifugation at 20380 x g at 4°C for 15 min, lysate supernatants were incubated with mNG-Trap agarose beads overnight at 4°C under gentle rotation. The beads were collected and washed three times with HEPES-RIPA buffer. Immunoprecipitants were eluted from the beads by boiling with 2x sample buffer at 95°C for 5 min.

For anti-FLAG M2 Magnetic Beads (M8823, Sigma) immunoprecipitated assay, HeLa cells expressing FLAG-protein were washed with TBS buffer [50mM Tris-HCl (pH 7.4), 150mM NaCl] twice and then lysed with lysis buffer [50 mM Tris-HCl (pH 7.4), 150 mM NaCl, 1 mM EDTA, 1% TritonX-100] containing 1x protease inhibitor cocktail. After 10 min

incubation on ice, cell lysates were centrifuged at 20380 x g for 10 min at 4°C. Collected supernatants were immunoprecipitated by anti-FLAG M2 Magnetic Beads for overnight at 4°C. After incubation, beads were washed with lysis buffer three times and TBS buffer twice, and then analyzed by immunoblotting. Immunoprecipitants were eluted from the beads by boiling with 2x sample buffer at 95°C for 5 min.

Lysosomal calcium measurement

Cells were loaded with 20 μM Oregon Green 488 BAPTA-5N (O6812, Invitrogen) and 0.25 mg/mL Texas Red 10 kD–conjugated dextran at 37°C in the culture medium for 16 h to allow the lysosomal accumulation of dyes through endocytosis. The medium was then changed to calcium-free Kreb's-Ringer solution containing 120 mM NaCl, 5 mM KCl, 1 mM $MgCl_2$, 25 mM $NaHCO_3$, and 5.5 mM D-glucose with ethanol or 1 mM LLOMe for confocal microscopy. Images were taken using an IX83 inverted microscope (Olympus) equipped with the Dragonfly 200 confocal system (Andor) and Fusion software (version 2.3.0.5.0). The fluorescence intensity of Oregon Green 488 BAPTA-5N was normalized to the fluorescence intensity of dextran using ImageJ/Fiji (National Institutes of Health). Calcium dynamics were assessed using F_{30}–F_0 analysis, defined as the difference in normalized fluorescence at 30 min minus the initial fluorescence (F_0). F_0 was defined as the time when ethanol or LLOMe was added, for a single cell with thresholded lysosomes depicted as a region of interest.

Correlative light electron microscopy (CLEM)

Cells were grown on the gridded 35 mm glass bottom dishes (P35G-2-14-CGRD, Mat-Tek). After transfection of siRNA and treatment with or without LLOMe, cells were fixed with 4% formaldehyde in 0.1 M phosphate buffer (pH 7.4) at room temperature and washed three times in the same buffer with 4% sucrose. Fixed cells were incubated for 30 min with DAPI. Fluorescent images of the target cells were captured on FV3000 confocal microscope, and DIC images of the same cells were also taken with letters around the target cells on the glass bottom to confirm the location of the cell in the dish. Cells were additionally fixed for 1 h with 1% formaldehyde and 1% glutaraldehyde in 0.1 M phosphate buffer, washed in the same buffer containing 4% sucrose, post-fixed for 60 min with 1% osmium tetroxide and 0.8% potassium ferrocyanide in 0.1 M phosphate buffer (pH7.4), washed in H2O, dehydrated in graded series of ethanol and embedded in a plastic cup which is 8 mm diameter filled with Epon 812 (TAAB Co. Ltd., UK) resin. 80 nm ultra thin

sections containing the target cell were stained with saturated uranyl acetate and Reynolds lead citrate solution.Electron micrographs were captured on a CCD camera Olympus Veleta 2K x 2K side-mounted on a JEM-1400plus transmission electron microscope (JEOL, Japan) at 80kV.

Measurement of SPLICS^{LY-MT}

HeLa cells stably expressing pMRX-ib-SPLICS^{LY-MT} were transfected with siLuc or siHKDC1. After 48 h, cells were treated with or without 1mM LLOMe for 2 h, and then fixed and mounted. Images were acquired in a series of 0.3 μm z-stacks using FV3000 confocal microscope. Pictures were processed and analyzed using Fiji software as previously described(1).

PLA

The PLA was performed using the Duolink in situ detection reagents Red (DUO92008, Sigma). Briefly, fixed cells were incubated with indicated antibodies in the corresponding figure legends for 1 h at room temperature and then incubated with PLA probe anti–rabbit MINUS (DUO92005, Sigma) and PLA probe anti–mouse PLUS (DUO92001, Sigma) at 37°C for 1 h. Images were taken using an FV3000 confocal microscope (Olympus) equipped with FV31S-SW software.

SA-β-gal staining

SA-β-gal staining was performed by using the Senescence Cells Histochemical Staining Kit (CS0030, Sigma). Briefly, cells were fixed with fixation buffer for 7 min at room temperature and stained with staining mixture at 37°C for 24 h without CO_2. The cells were observed using a BX53 microscope (Olympus) and images were captured using cellSens Standard (version 1.16).

Measurement of reactive oxygen species (ROS)

The level of ROS accumulation was detected by MitoSOX (M36008, Molecular Probes). Briefly, after the incubation with 5μM MitoSOX for 10 min at 37°C, RPE1 cells were washed HBSS buffer and mounted in JC-1 imaging buffer (MT09, Dojindo) to detect the signals using CQ1.

Measurement of oxygen consumption rate (OCR)

OCR was measured in RPE1 cells with a Seahorse XFe extracellular flux analyzer (Agilent Technologies) according to the manufacturer's instructions. Briefly, RPE1 cells were cultured in Seahorse XF DMEM medium, pH 7.4 (103575-100, Agilent Technologies) supplemented with 10 mM glucose (103577-100, Agilent Technologies), 1 mM pyruvate (103578-100, Agilent Technologies), and 2 mM L-glutamine (103579-100, Agilent Technologies) for 1 h at 37°C without CO_2, and subsequently stimulated with Oligomycin (1.5 μM), FCCP (2 μM), and Rotenone/Antimycin A (0.5 μM) (103015-100, XF Cell Mito Stress Test Kit, Agilent Technologies) to determine mitochondrial activity. Cellular OCR was analyzed with Wave software v2.6.3 (Agilent Technologies).

Data and code availability

RNA-seq data used in this study have been deposited to the National Center for Biotechnology Information Gene Expression Omnibus with accession number GSE226743. Proteomic data have been deposited through Proteome Xchange (jPOST), with accession numbers of PXD040970 for ProteomeXchange and JPST002097 for jPOST. This paper does not report original code.

Quantification and statistical analysis

Protein levels were quantified using ImageJ/Fiji. Statistical analyses and data plotting were performed using GraphPad Prism software (version 9.5.0). Statistical details of experiments can be found in the corresponding figure legends.

SI Figures

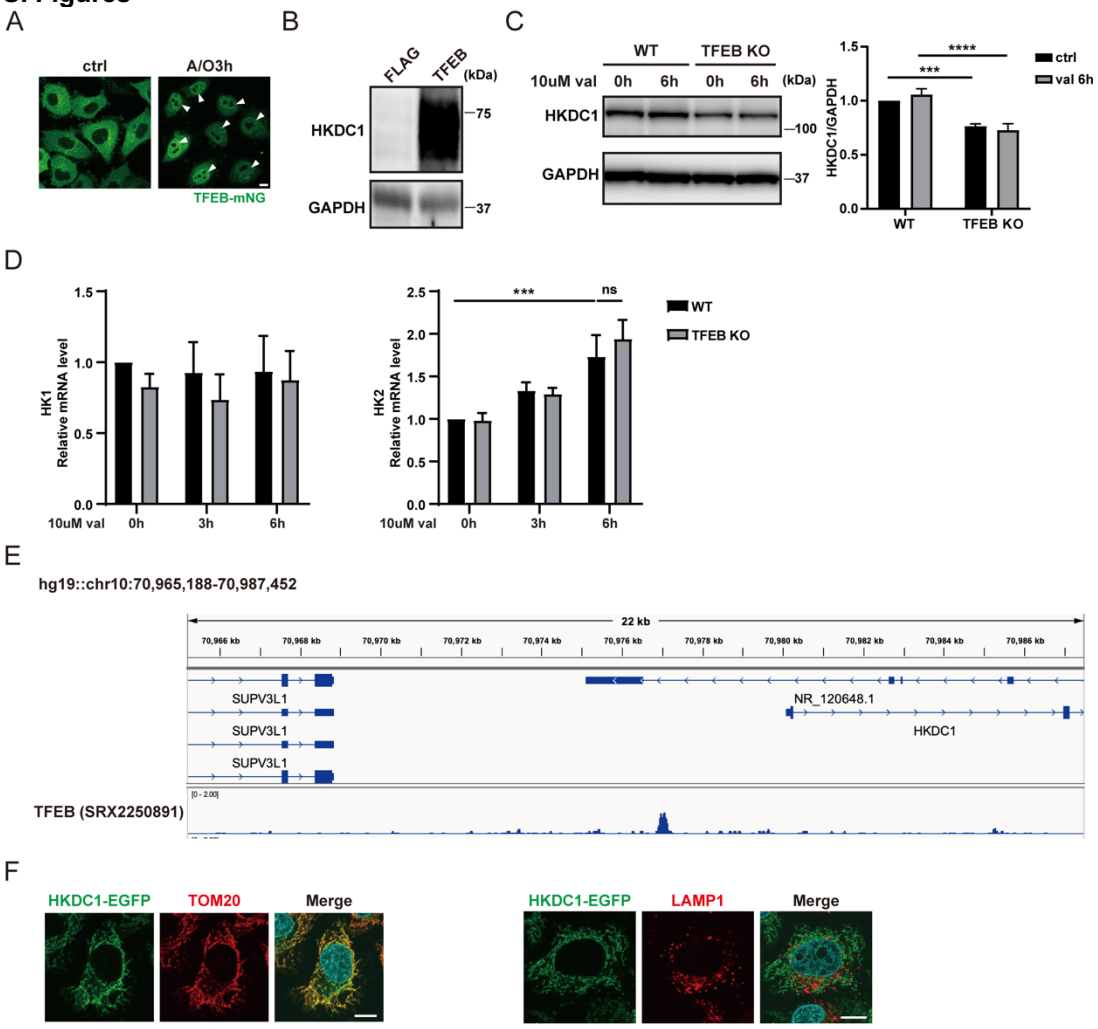

Fig. S1. *HKDC1* deficiency impairs PINK1/Parkin-mediated mitophagy. Related to Figure 1.

A. Representative IF images of TFEB-mNG in the HeLa cells stably expressing TFEB-mNG, treated with or without A/O for 3 h. White arrowheads indicate nuclear localized TFEB. Scale bar, 10 μm.

B. Representative WB of TFEB in 3xFLAG or TFEB-3xFLAG expressing HeLa cells.

C. Representative WB (left) and quantification (right) of HKDC1 in WT or TFEB KO HeLa cells with 10 μM val treatment for 0 h and 6 h. N=3.

D. Relative mRNA expression of HK1 and HK2 in WT or TFEB KO HeLa cells treated with 10 μM val for 0 h, 3 h, or 6 h. Data were normalized by GAPDH and are expressed relative to WT untreated with val. N=3.

E. HKDC1 loci are shown in the IGV genome browser, with TFEB ChIP-seq data (SRX2250891) visualized with ChIP-Atlas.

F. Representative images of HeLa cells transiently expressing HKDC1-EGFP, as detected by IF staining with mitochondrial marker TOM20 or lysosomal marker LAMP1(as a negative control). Scale bar, 10 μm. Values are represented as the mean ± SD, and p-values (***p<0.001, ****p<0.0001) were determined by one-way analysis of variance (ANOVA) with Tukey's multiple comparison test.

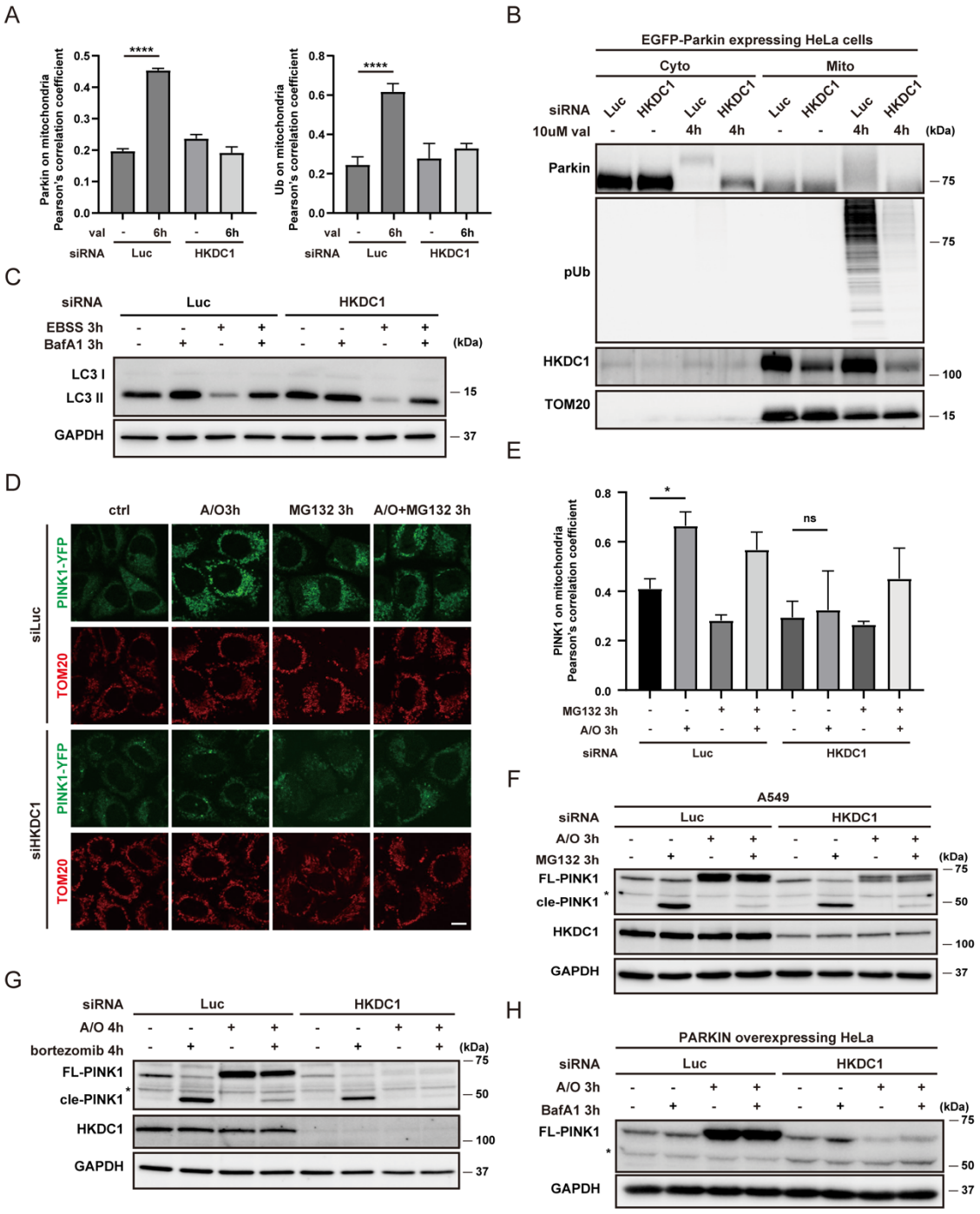

Fig. S2. HKDC1 deficiency impairs PINK1/Parkin-mediated mitophagy. Related to Figure 2.

A. Quantification of EGFP-Parkin or endogenous Ub on mitochondria (Figure 2B) in siLuc- or siHKDC1-transfected HeLa cells treated with or without 10 μM val for 6 h. N=3.

B. Representative WB of Parkin, pUb, HKDC1 and TOM20 of the cytosol-rich fraction and mitochondria-rich fraction extracted from siLuc- or siHKDC1-transfected HeLa cells treated with or without 10 μM val for 4 h.

C. Representative WB of LC3 autophagic flux in siLuc- or siHKDC1-transfected HeLa cells treated with or without EBSS or 125 nM BafA1 for 3 h.

D.E. Representative IF images (D) and quantification (E) of PINK1-YFP on mitochondria in siLuc- or siHKDC1-transfected PINK1 KO HeLa cells expressing PINK1-YFP treated with or without A/O and 10 μM MG132 for 3 h. N=3. Scale bar, 10 μm

F. Representative WB of FL-PINK1 and cle-PINK1 in A549 cells treated with or without A/O and 10 μM MG132 for 3 h. Asterisk denotes non-specific bands.

G. Representative WB of FL-PINK1 and cle-PINK1 in siLuc- or siHKDC1-transfected HeLa cells treated with or without A/O and 10 μM bortezomib for 4 h. Asterisk denotes non-specific bands.

H. Representative WB of FL-PINK1 in siLuc- or siHKDC1-transfected HeLa cells overexpressing EGFP-Parkin treated with or without A/O and 125 nM BafA1 for 3 h. Asterisk denotes non-specific bands. Values are represented as the mean ± SD, and p-values (*$p<0.05$, ****$p<0.0001$) were determined by one-way analysis of variance (ANOVA) with Tukey's multiple comparison test.

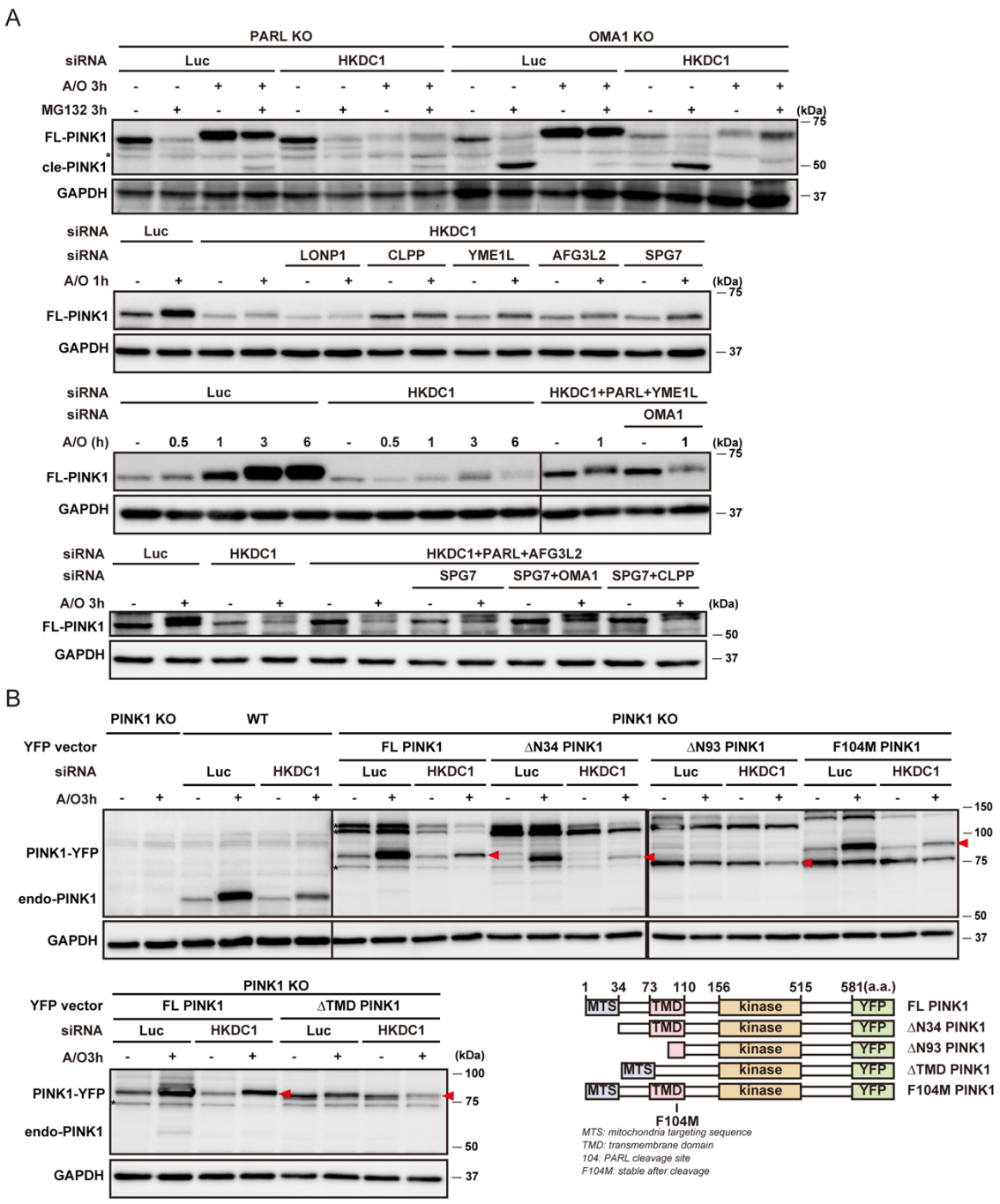

Fig. S3. HKDC1 deficiency impairs PINK1/Parkin-mediated mitophagy. Related to Figure 2.

A. Representative WB of FL-PINK1 and cle-PINK1 in normal or HKDC1-deficient HeLa cells with or without knockout of PARL or OMA1 or knockdown of several mitochondrial protease genes and treated with or without A/O for 1 h or 3 h and MG132 for 3 h. Asterisk denotes non-specific bands.

B. Representative WB of PINK1-YFP and endogenous PINK1 (endo-PINK1) in normal or PINK1 KO HeLa cells with or without several stably expressed PINK1 variants and treated with or without A/O for 3 h. Red arrowheads represent the bands of PINK1 variants and asterisks denote non-specific bands. The lower right panel shows the schematic domain structure of a PINK1 mutant with an N-terminal MTS site, transmembrane domain (TMD), kinase domain, and YFP tag.

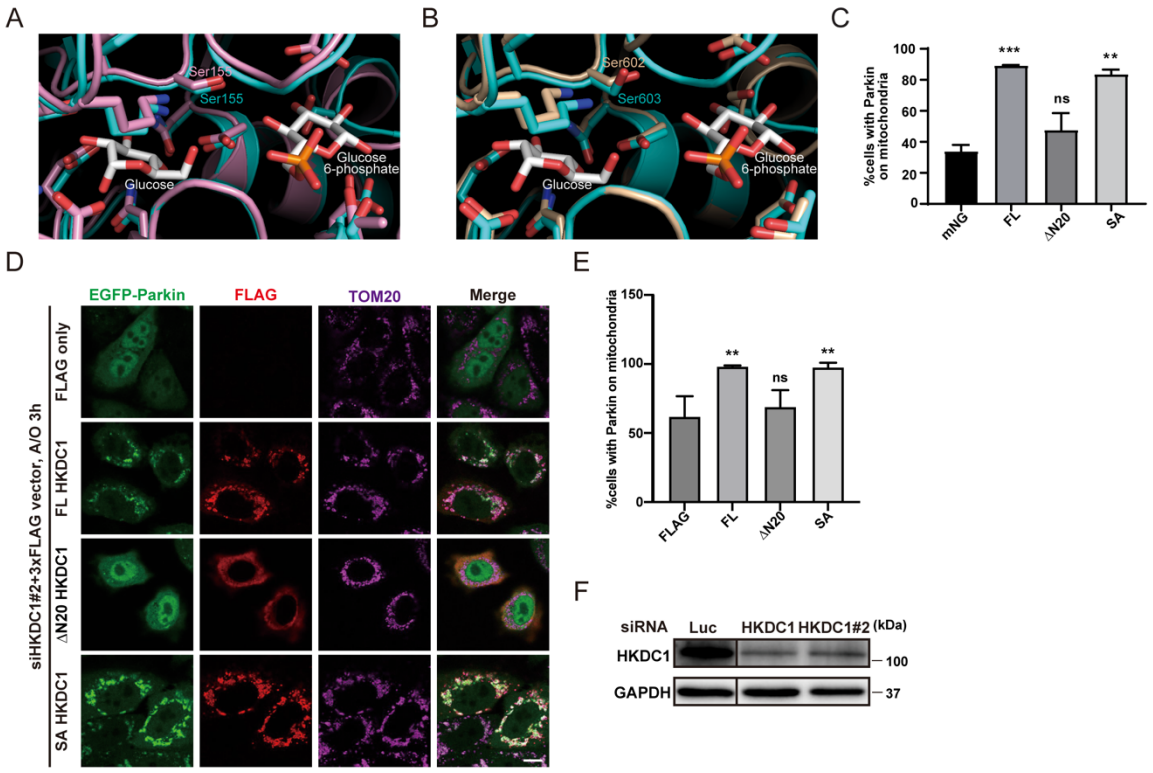

Fig. S4. Localization of HKDC1 in mitochondria is required for PINK1 accumulation and Parkin recruitment. Related to Figure 3.

A.B. The active sites of the HKDC1 and HK2 hexokinase domains exhibit a substantial structural similarity. The N- and C-terminal domains of HKDC1 (AF-Q2TB90-F1-model_v4) are colored in pink (A) and wheat (B), respectively, while HK2 and the glucose and glucose 6-phosphate molecules bound to HK2 (2NZT) are in cyan and white, respectively. Besides the ligands, residues annotated to be important for their binding are depicted in sticks, including the Ser residues mutated to Ala for HKDC1 (this study) and HK2. Water molecules are not shown for clarity.

C. Quantification of mNG-HKDC1, Myc-Parkin, and TOM20 detected by IF (Figure 3B) in siHKDC1 HeLa cells overexpressing mNG, FL HKDC1-mNG, ΔN20 HKDC1-mNG, or SA HKDC1-mNG, and treated with A/O for 3 h. N=3.

D.E. Representative images (D) and quantification (E) of FLAG, EGFP-Parkin, and TOM20 detected by IF in siHKDC1#2 HeLa cells overexpressing 3xFLAG, FL HKDC1-3xFLAG, ΔN20 HKDC1-3xFLAG, or SA HKDC1-3xFLAG, and treated with A/O for 3 h. N=3. Scale bar, 10 μm.

F. Representative WB of HKDC1 in siLuc- or siHKDC1- or siHKDC1#2-transfected HeLa cells. Values are represented as the mean ± SD, and p-values (**p<0.01, ***p<0.001) were determined by one-way ANOVA with Tukey's multiple comparison test.

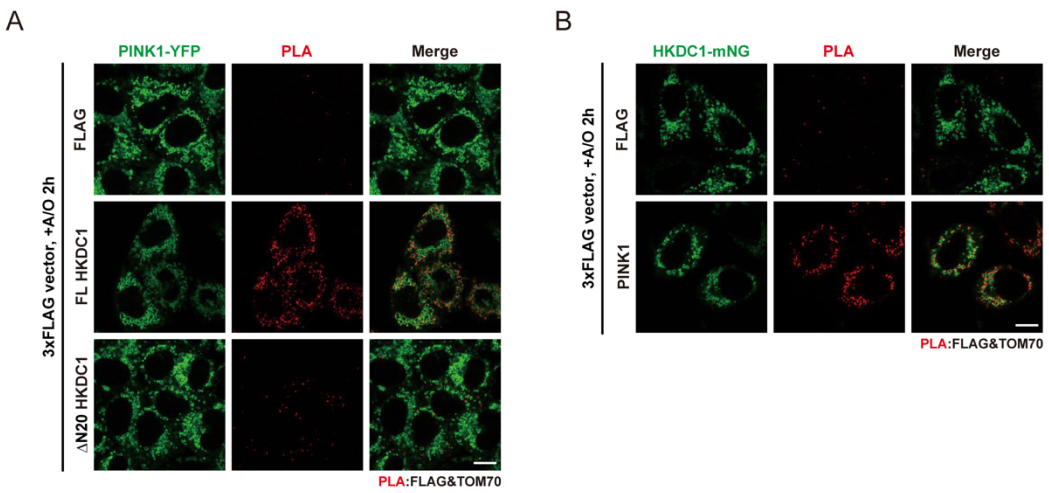

Fig. S5. **HKDC1 interacts with the PINK1 import receptor TOM70 on mitochondria. Related to Figure 4.**

A. Representative images of PINK1-YFP and interaction between HKDC1 and TOM70, determined using PLA. The PLA signals were detected by FLAG and TOM70 antibody in HeLa cells transiently expressing 3xFLAG, FL HKDC1-3xFLAG or ND HKDC1-3xFLAG, treated with A/O for 2 h. Scale bar, 10 μm.

B. Representative images of HKDC1-mNG and interaction between PINK1 and TOM70, determined using PLA. The PLA signals were detected by FLAG and TOM70 antibody in HeLa cells expressing HKDC1-mNG, and 3xFLAG or PINK1-3xFLAG, treated with A/O for 2 h. Scale bar, 10 μm.

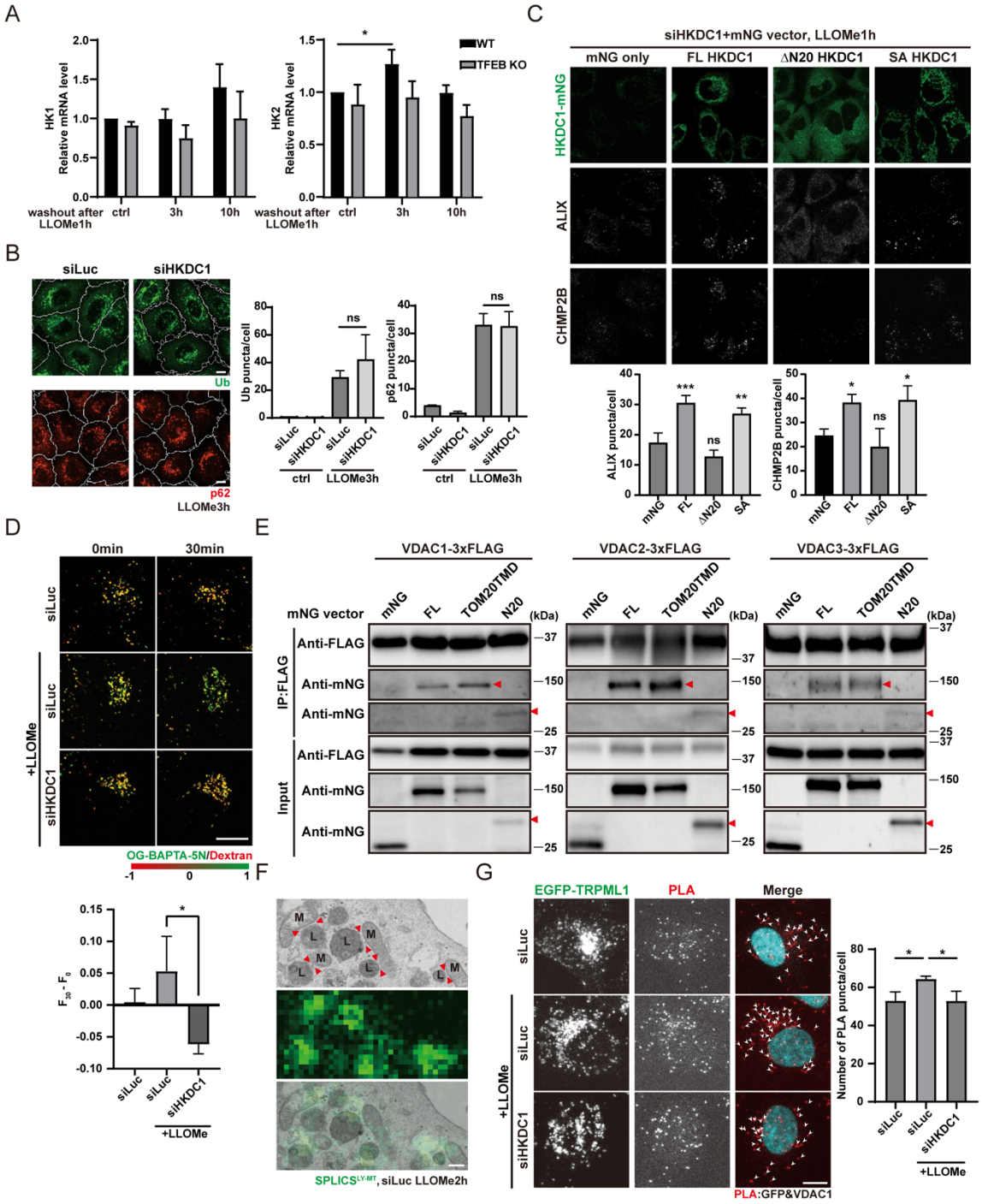

Fig. S6. The regulation of mitochondria–lysosome contact by complexes of HKDC1 with VDACs is essential for lysosomal recovery. Related to Figure 5.

A. Relative mRNA expression of HK1 and HK2 in WT or TFEB KO HeLa cells with or without 1 mM LLOMe treatment for 1 h, followed by washout for 3 h or 10 h. N=3.

B. Representative images of Ub or p62 puncta in siLuc- or siHKDC1-transfected HeLa cells treated with 1 mM LLOMe for 3 h (left) detected by IF. Quantification of Ub or p62 puncta per cell (right). N=3. Scale bar, 10 μm.

C. Representative images (upper) and quantification (lower) of ALIX and CHMP2B in HKDC1 knockdown HeLa cells expressing mNG, FL HKDC1-mNG, △N20 HKDC1-mNG, or SA HKDC1-mNG, treated with 1 mM LLOMe for 1 h. N=3. Scale bar, 10 μm.

D. Representative images (left) and quantification (right) of lysosomal calcium signals detected by Oregon Green 488 BAPTA-5N (OG-BAPTA-5N) and normalized by dextran signals from three independent experiments each analyzing 10 cells. $F_{30} - F_0$ represents the normalized fluorescence of lysosomal calcium after continuous LLOMe treatment for 30 min minus the fluorescence at the initial time point. N=3. Scale bar, 10 μm.

E. Representative immunoblots of FLAG and mNG in EGFP-Parkin–expressing HeLa cells transiently expressing TOM70-3xFLAG and mNG, FL HKDC1-mNG, TOM20TMD HKDC1-mNG, or N20 HKDC1-mNG followed by immunoprecipitation with antibody against FLAG. Red arrowheads denote TOM20TMD HKDC1-mNG or N20 HKDC1-mNG.

F. Representative correlative light electron microscopy of lysosomes containing electron-dense lumen forming contact sites with mitochondria showing the morphology of the cristae in HeLa cells expressing $SPLICS^{LY\text{-}MT}$. Red arrowheads represent contact sites. Sclae bar, 200nm.

G. Representative images (left) and quantification (right) of interaction between EGFP-TRPML1 and VDAC1, determined using PLA. The PLA signals were detected by GFP and VDAC1 antibody. Nuclei were stained with DAPI. White arrowheads represent PLA puncta. N=3. Scale bar, 10 μm. Values are represented as the mean ± SD, and p-values (*p<0.05, **p<0.01, ***p<0.001) were determined by one-way analysis of variance (ANOVA) with Tukey's multiple comparison test.

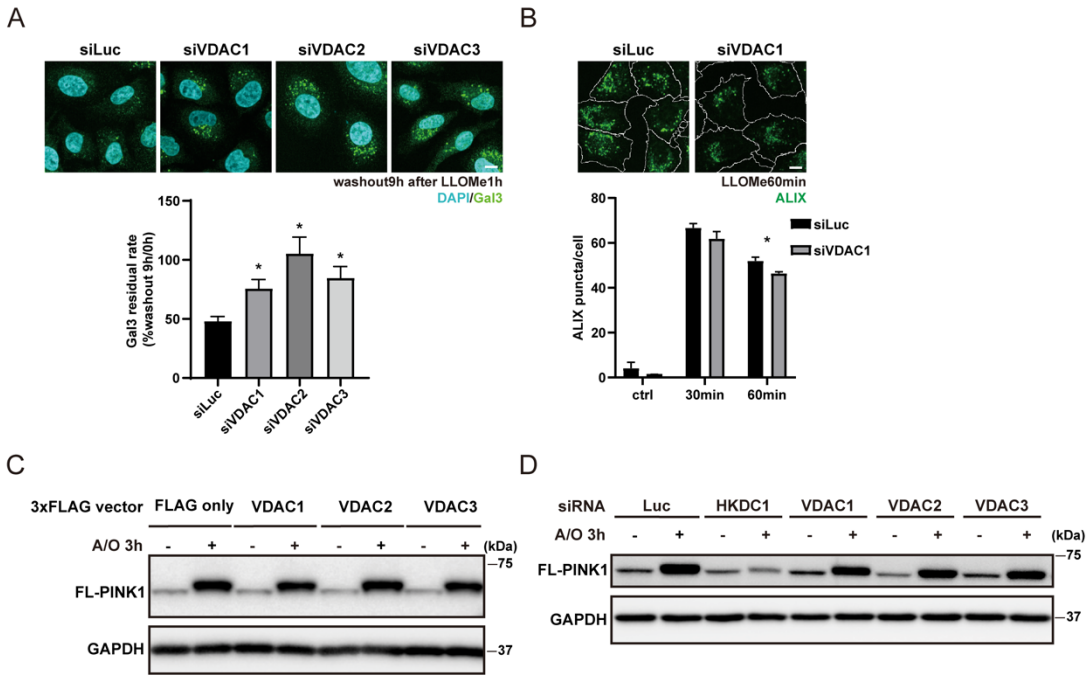

Fig. S7. **The regulation of mitochondria–lysosome contact by complexes of HKDC1 with VDACs is essential for lysosomal recovery. Related to Figure 5.**

A. Representative images (upper) and quantification (lower) of damaged lysosomes in VDACs knockdown HeLa cells treated with LLOMe for 1 h, followed by washout for 9 h and determined by immunostaining with Gal3 antibody. N=3. Scale bar, 10 μm.

B. Representative images of ALIX puncta in siLuc- or siVDAC1-transfected HeLa cells treated with 1 mM LLOMe for 60 min (upper) detected by IF. Quantification of ALIX puncta per cell in siLuc- or siVDAC1-transfected HeLa cells treated with 1 mM LLOMe for 0 min, 30 min or 60 min (lower). N=3. Scale bar, 10 μm.

C. Representative WB of FL-PINK1 in HeLa cells overexpressing control 3xFLAG or VDAC1-, VDAC2-, or VDAC3-3xFLAG, and treated with or without A/O for 3 h.

D. Representative WB of FL-PINK1 in siLuc-, siHKDC1-, and siVDAC1-, 2-, and 3-transfected HeLa cells treated with or without A/O for 3 h. Values are represented as the mean ± SD, and p-values (*p<0.05) were determined by one-way ANOVA with Tukey's multiple comparison test.

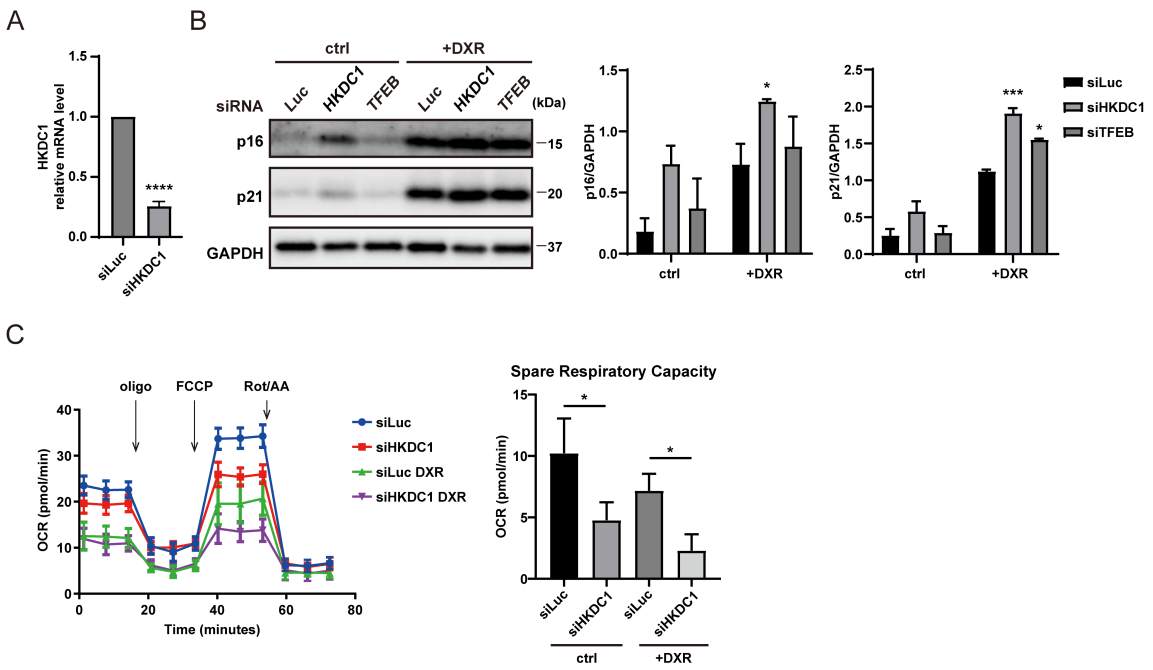

Fig. S8. Mitochondrial and lysosomal homeostasis maintained by HKDC1 counteracts cellular senescence. Related to Figure 6.

A. qPCR-determined relative mRNA expression of HKDC1 in HKDC1 knockdown RPE1 cells. N=3.

B. Representative WB (left) and quantification (right) of p16 and p21 in siLuc-, siHKDC1-, or siTFEB-transfected RPE1 cells treated with or without 150 ng/mL DXR for 3 d. N=3.

C. Representative OCR profile (left) and spare respiratory capacity (right) of siLuc- or siHKDC1-transfected RPE1 cells with or without 50 ng/mL DXR for 2 d. The metabolic inhibitors, oligomycin (oligo), FCCP and rotenone/antimycin A (Rot/AA) were injected at the indicated time points. N=3. Values are represented as the mean ± SD, and *p*-values (*p<0.05, ***p<0.001, ***p<0.0001) were determined by one-way ANOVA with Tukey's multiple comparison test (B, C) or unpaired t-test (A).

Full blots

Fig1c HKDC1

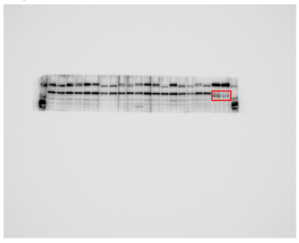

Fig1c GAPDH

Fig2a UQCRC1

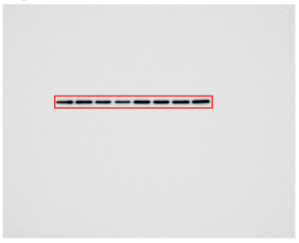

Fig2a TOM20

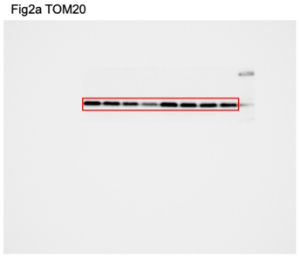

Fig2a HKDC1

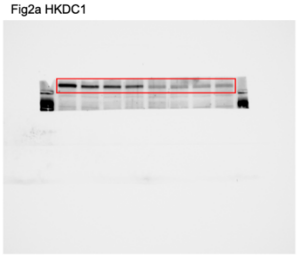

Fig2a GAPDH

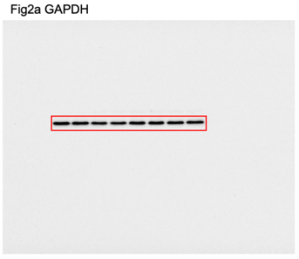

Fig2c pUb

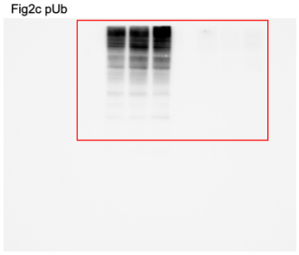

Fig2d PINK1

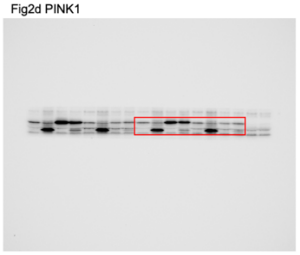

Fig2d GAPDH

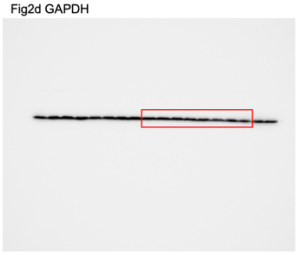

Fig2f PINK1

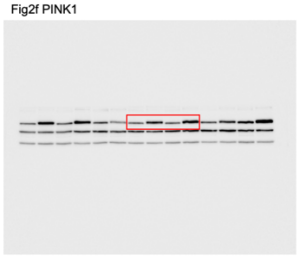

Fig2f HKDC1

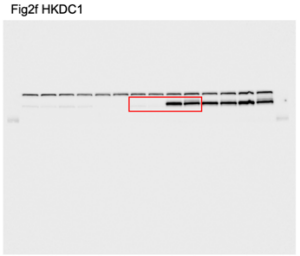

Fig2f GAPDH

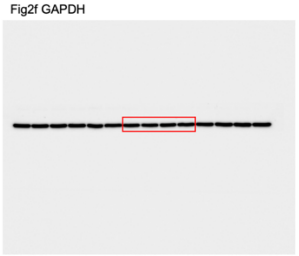

Fig2g PINK1

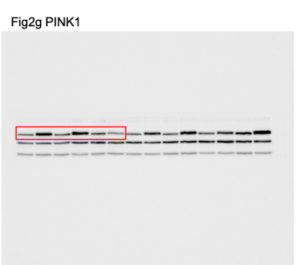

Fig2g HKDC1

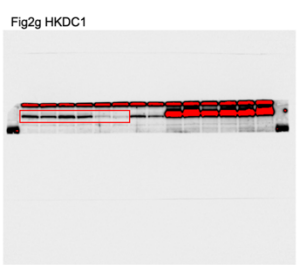

Fig2g GAPDH

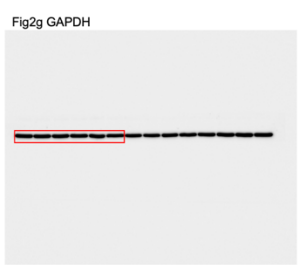

Fig3c PINK1

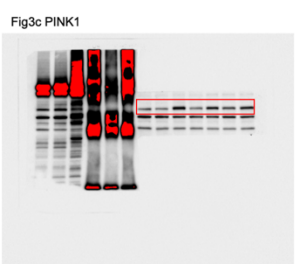

Fig3c HKDC1

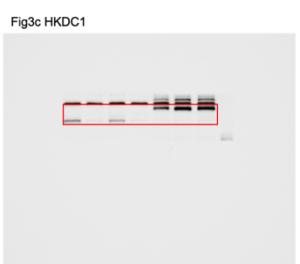

Fig3c GAPDH

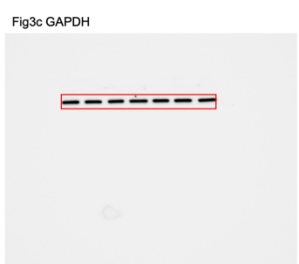

Fig4c FLAG Input

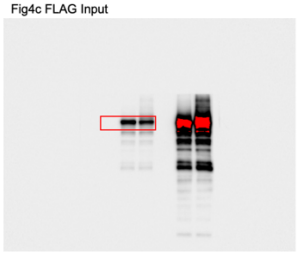

Fig4c PINK1 Input

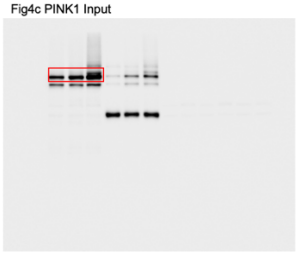

Fig4c TOM70 Input

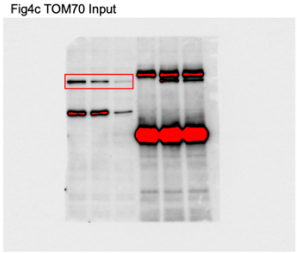

Fig4c FLAG IP

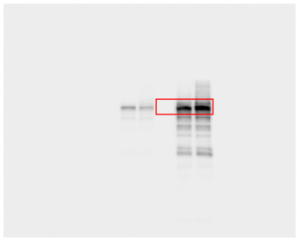

Fig4c PINK1 IP

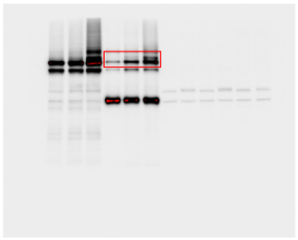

Fig4c TOM70 IP

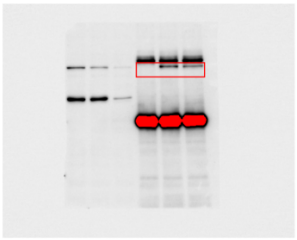

Fig4d TOM70

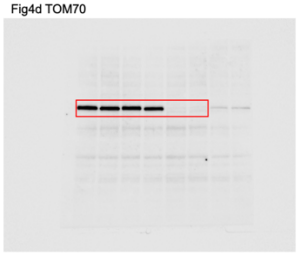

Fig4d PINK1

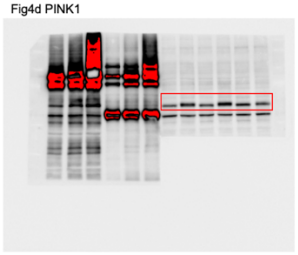

Fig4d GAPDH

Fig4f FLAG Input

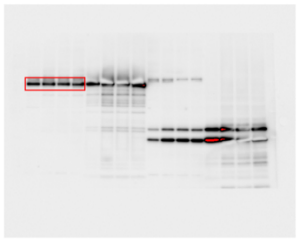

Fig4f FLAG IP

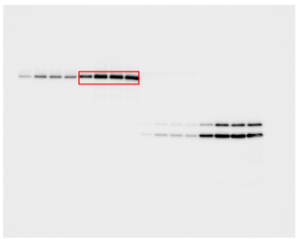

Fig4f mNG Input and IP

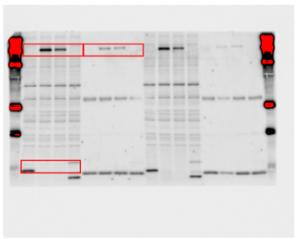

Fig4f mNG IP

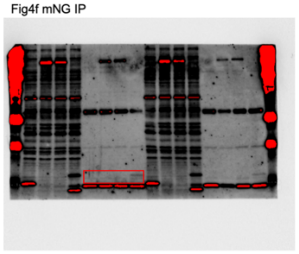

Fig5e FLAG Input

Fig5e FLAG IP

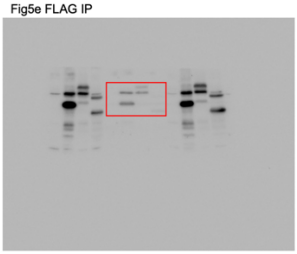

Fig5e mNG Input

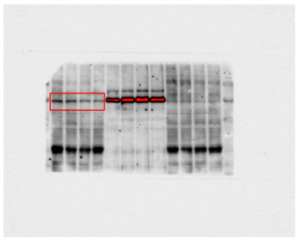

Fig5e mNG IP

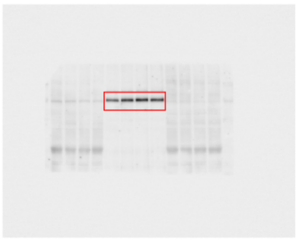

Fig6b GAPDH

Fig6b p16

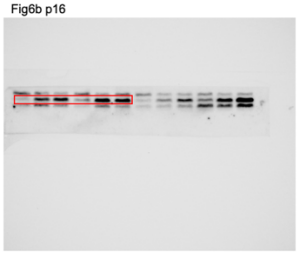

Fig6b p21

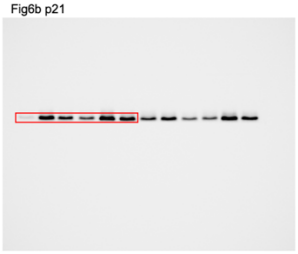

Fig6f GAPDH

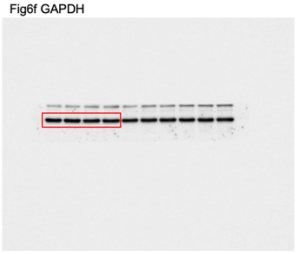

Fig6f TOM20

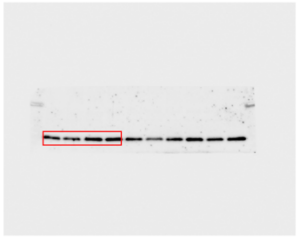

Fig6f UQCRC1

FigS1a TFEB

FigS1a GAPDH

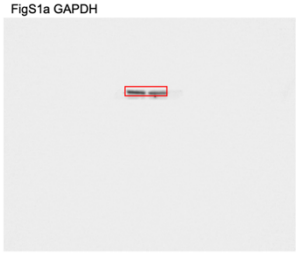

FigS1b HKDC1

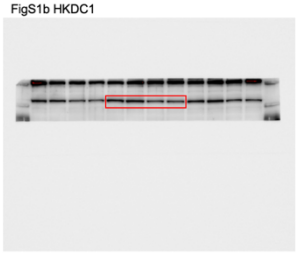

FigS1b GAPDH

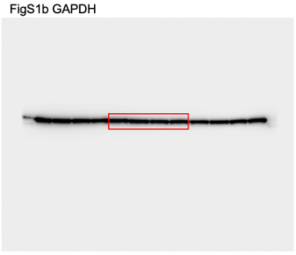

FigS2b pUb

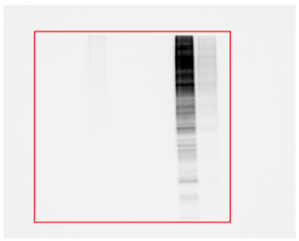

FigS2b Parkin

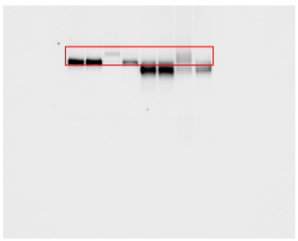

FigS2b TOM20

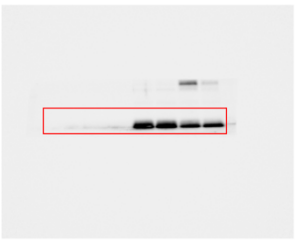

FigS2b HKDC1

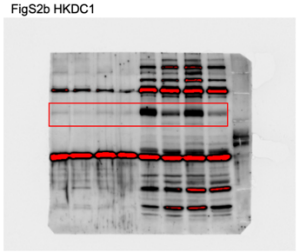

FigS2c LC3

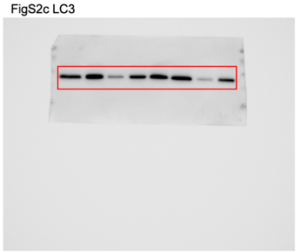

FigS2c GAPDH

FigS2f PINK1

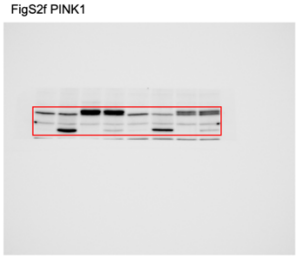

FigS2f HKDC1

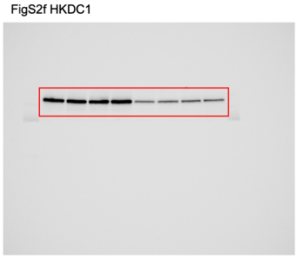

FigS2f GAPDH

FigS2g PINK1

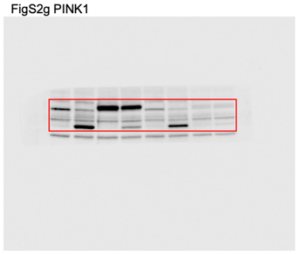

FigS2g HKDC1

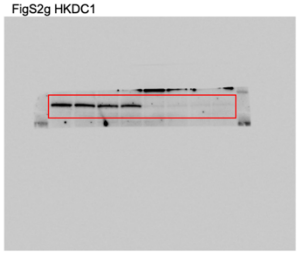

FigS2g GAPDH

FigS2h PINK1

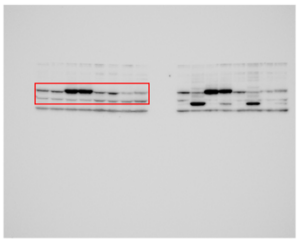

FigS2h PNIK1

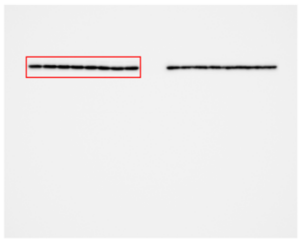

FigS3a PINK1-1

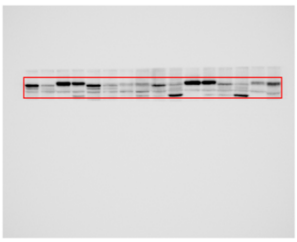

FigS3a GAPDH-1

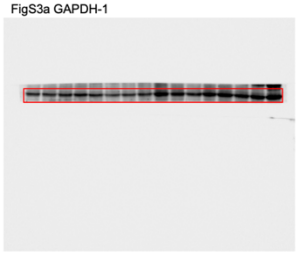

FigS3a PINK1-2

FigS3a GAPDH-2

FigS3a PINK1-3

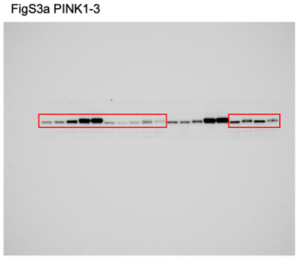

FigS3a GAPDH-3

FigS3a PINK1-4

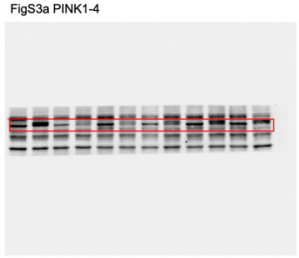

FigS3a GAPDH-4

FigS3b PINK1-1

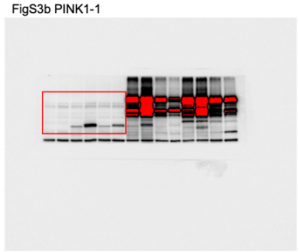

FigS3b PINK1-2

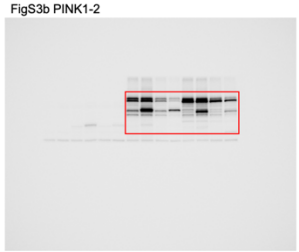

FigS3b GAPDH-1&2

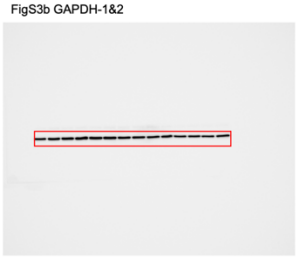

FigS3b PINK1-3

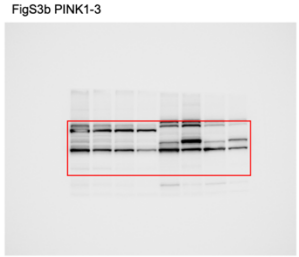

FigS3b GAPDH-3

FigS3b PINK1-4

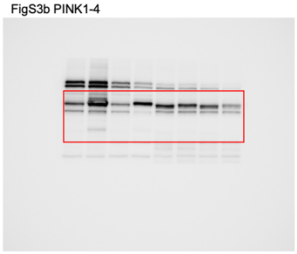

FigS3b GAPDH-4

FigS4f HKDC1

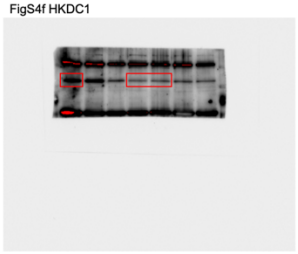

FigS4f GAPDH

FigS6e FLAG Input-1

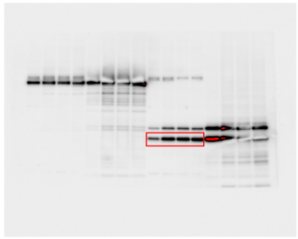

FigS6e FLAG IP-1

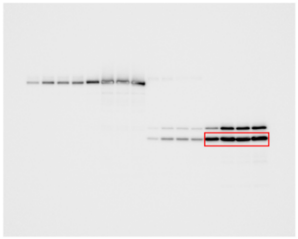

FigS6e mNG Input-1

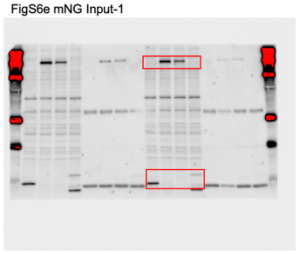

FigS6e mNG IP-1

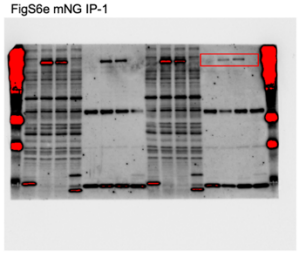

FigS6e mNG IP-1

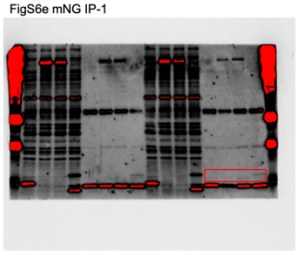

FigS6e FLAG Input&IP-2

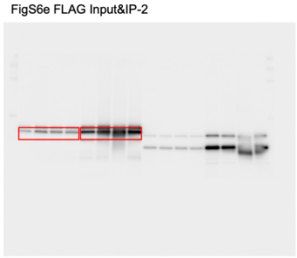

FigS6e mNG Input-2

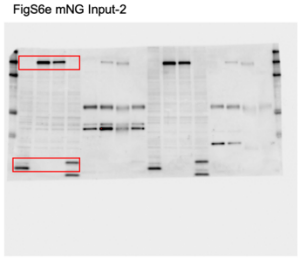

FigS6e mNG IP-2

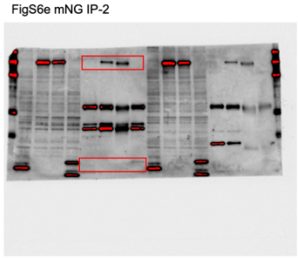

FigS6e FLAG Input-3

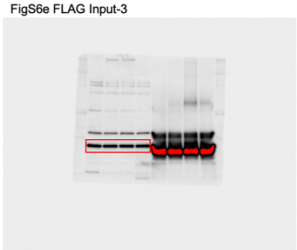

FigS6e FLAG IP-3

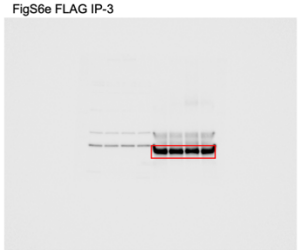

FigS6e mNG Input-3

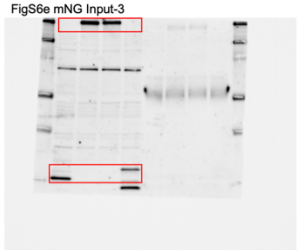

FigS6e mNG IP-3

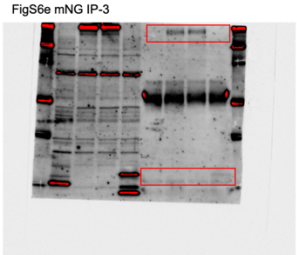

FigS7c PINK1

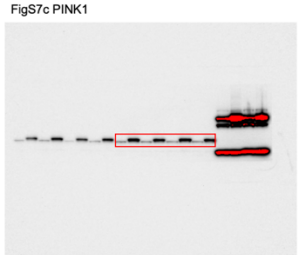

FigS7c GAPDH

FigS7d PINK1

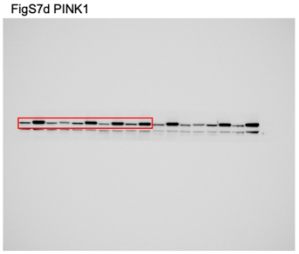

FigS7d GAPDH

FigS8b GAPDH

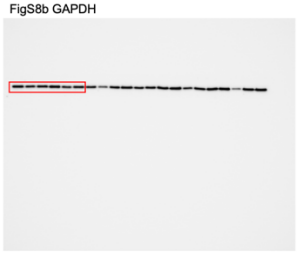

FigS8b p16

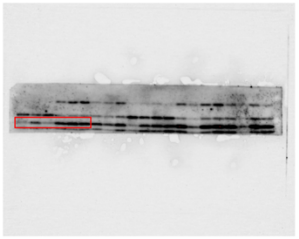

FigS8b p21

SI References

1. T. Cali, M. Brini, Quantification of organelle contact sites by split-GFP-based contact site sensors (SPLICS) in living cells. *Nat Protoc* **16**, 5287-5308 (2021).
2. K. Yamano *et al.*, Critical role of mitochondrial ubiquitination and the OPTN-ATG9A axis in mitophagy. *J Cell Biol* **219** (2020).
3. Y. Oe *et al.*, PACSIN1 is indispensable for amphisome-lysosome fusion during basal autophagy and subsets of selective autophagy. *PLoS Genet* **18**, e1010264 (2022).
4. T. Saitoh *et al.*, TWEAK induces NF-kappaB2 p100 processing and long lasting NF-kappaB activation. *J Biol Chem* **278**, 36005-36012 (2003).
5. A. M. Bolger, M. Lohse, B. Usadel, Trimmomatic: a flexible trimmer for Illumina sequence data. *Bioinformatics* **30**, 2114-2120 (2014).
6. D. Kim *et al.*, TopHat2: accurate alignment of transcriptomes in the presence of insertions, deletions and gene fusions. *Genome Biol* **14**, R36 (2013).
7. M. D. Robinson, D. J. McCarthy, G. K. Smyth, edgeR: a Bioconductor package for differential expression analysis of digital gene expression data. *Bioinformatics* **26**, 139-140 (2010).
8. M. Tsuchiya *et al.*, Exportin 4 interacts with Sox9 through the HMG Box and inhibits the DNA binding of Sox9. *PLoS One* **6**, e25694 (2011).
9. J. Jumper *et al.*, Highly accurate protein structure prediction with AlphaFold. *Nature* **596**, 583-589 (2021).
10. M. Varadi *et al.*, AlphaFold Protein Structure Database: massively expanding the structural coverage of protein-sequence space with high-accuracy models. *Nucleic Acids Res* **50**, D439-D444 (2022).
11. M. H. Nawaz *et al.*, The catalytic inactivation of the N-half of human hexokinase 2 and structural and biochemical characterization of its mitochondrial conformation. *Biosci Rep* **38** (2018).